

Cesium adsorption on TiO₂(110)

Ann W. Grant and Charles T. Campbell

Chemistry Department, Box 351700, University of Washington, Seattle, Washington 98195-1700

(Received 2 August 1996)

The adsorption of Cs on a TiO₂(110) rutile surface was investigated at 130–800 K using x-ray photoelectron spectroscopy, x-ray excited Auger electron spectroscopy, temperature-programmed desorption, work-function, and band-bending measurements. Below room temperature, the Cs displays a Stranski-Krastanov growth mode, with the completion of a uniform monolayer (ML) containing $(6 \pm 2) \times 10^{14}$ Cs adatoms per cm², followed by the growth of three-dimensional clusters of Cs that cover only a small fraction of the surface. The Cs in the first $\sim \frac{1}{2}$ ML is very cationic, donating electron density to the TiO₂. Most of this charge is localized near the topmost atomic layers, with Ti⁴⁺ ions being reduced to Ti³⁺. This gives rise to a local dipole moment of the adsorbate-substrate complex of ~ 6 D at ~ 0.1 ML. However, a small part of the charge transferred to the substrate also goes much deeper into the solid, giving rise to downward band bending of ~ 0.2 – 0.3 eV. This band bending nearly saturates at ~ 0.05 ML. The local dipole moment of the alkali-metal–substrate complex decreases smoothly with coverage in the first ML, due to dipole-dipole repulsions and their consequent mutual depolarization, similar to transition-metal surfaces. This gives rise to a rapid and smooth decrease in the heat of adsorption with coverage from >208 kJ/mol down to ~ 78 kJ/mol. [S0163-1829(97)02604-0]

I. INTRODUCTION

The adsorption of alkali metals on oxide surfaces is important in catalysis, where alkali metals are often added as promoters to solid catalysts consisting mainly of oxide particles. In addition, their adsorption is important in environmental chemistry and geological problems, where alkali-metal adsorption on oxides occurs during wastewater cleanup, and in mineral growth. Nevertheless, studies of alkali-metal adsorption on clean and well-defined oxide surfaces using surface-sensitive characterization techniques are still relatively few.

Those few prior studies show that when alkali-metal vapor is adsorbed onto a clean oxide surface, a first monolayer is usually formed which covers all or most of the surface before three-dimensional growth begins.^{1–21} Electron spectroscopic methods have often led to the conclusion that a large fraction of this first monolayer is strongly cationic in electronic character.^{2,3,5,7,8,10,15} In one unusual case, a Volmer-Weber growth mode (three-dimensional particles well before monolayer completion) was proposed for alkali-metal adsorption, in that case to explain Auger electron spectroscopy (AES) data and the lack of low-energy electron diffraction (LEED) structures for Na growth on MgO(001).²²

A specific overlayer structure [(2×2) , $c(4 \times 2)$, $c(2 \times 2)$, or $\sqrt{3}$] has been reported in many LEED studies of alkali metals at submonolayer coverages on oxide crystals.^{2,6,8–13} This shows that alkali-metal adatoms prefer to sit in specific surface sites offered by the oxide lattice, at least up to coverages of $\frac{1}{4}$ to $\frac{1}{2}$ monolayer. This conclusion is also supported by surface-extended x-ray-absorption fine structure (SEXAFS) and other measurements.^{9,11,23}

In this present work, we report a study of Cs adsorption on TiO₂(110) using x-ray photoelectron spectroscopy (XPS), temperature-programmed desorption (TPD), work-function, and band-bending measurements. We find that the Cs adsorbs cationically up to moderate coverages, but this con-

verts smoothly to metallic adsorption by one monolayer. There is a strong and continuous but smooth decrease in the desorption energy for the alkali metal as this transition to metallic adsorption occurs, which evolves ultimately to the sublimation energy of bulk Cs at coverages beyond one monolayer.

Work-function measurements have been performed in a few cases for alkali-metal adsorption on semiconducting oxide surfaces, but in those cases band-bending measurements were not simultaneously performed.^{2,10,15,17} A correction of the work-function curve for band bending is needed on semiconductors in order for the local surface dipole moment of the adsorbate-substrate complex to be accurately determined,^{1,24–26} as we do here for Cs on TiO₂(110).

Alkali-metal adsorption on oxides has also been studied by temperature-programmed desorption in a few cases.^{5,6,17,19,20} To our knowledge only one prior study has followed the adsorption process by TPD up to multilayer coverages of the alkali-metal as we do here, showing the transition from ionic to metallic adsorption.⁶ However, for that case of K on TiO₂(110), contradictory results were reported by Lad and Dake,⁵ who never saw the multilayer K desorption peak develop, even after very large doses of the alkali-metal.

II. EXPERIMENT

A two-chamber ultrahigh-vacuum system was used to perform these experiments, each chamber with a base pressure of 1×10^{-10} mbar. Details of this apparatus have been given previously.²⁷ The system had capabilities for TPD, XPS, Auger electron spectroscopy (AES), work function, and LEED.

The procedure for preparing and mounting the rutile TiO₂(110) single crystal and the sputtering/annealing procedure used to clean it have also been described previously.^{28,29} The cleaning procedure has been shown to produce a nearly

stoichiometric and well-ordered TiO₂(110) surface, which was checked with XPS and LEED. The unit cell of the TiO₂(110) surface has dimensions of 2.96 Å × 6.49 Å, giving 5.2 × 10¹⁴ unit cells per cm² of surface area.

Cesium was dosed to the front surface using a vapor deposition source, containing a Cs zeolite getter (SAES Getters, S.p.A.), which was resistively heated to ~863K to obtain the Cs vapor. This source has been described previously,³⁰ and the way it is mounted is similar to that described in Ref. 31. The ratio of the Cs(3d_{5/2}) to the clean Ti(2p_{3/2}) peak areas in XPS was used to quantify the amount of Cs dosed to the surface. The XPS signals were measured within a 6° cone of acceptance angles normal to the surface, always using Al Kα x rays.

The TPD experiments were performed using a heating rate of 4.25 K/s. Desorbed species were detected with a line-of-sight quadrupole mass spectrometer set at ~45° from the surface normal.

Work-function changes ($\Delta\phi$) were monitored by shifts in the low-energy onset of secondary electron distribution in the XPS spectrum, similar to that described previously,³⁰ with the sample biased at -14.25 V, using a low pass energy (20 eV) for high resolution. Band-bending measurements were performed using the Ti(2p_{3/2}) peak in normal XPS.

III. RESULTS

The process of repeatedly adsorbing Cs onto TiO₂(110), probing it by TPD, and then recleaning it rapidly led to the buildup of a form of Cs on the surface which was most difficult to remove by sputtering and annealing. For this reason, we performed most of the experiments here with a "clean" TiO₂(110) surface which actually contained a small residual Cs impurity. This typical residual "background" Cs signal in XPS is shown as curve *a* in Fig. 1. This level of Cs was typically obtained by sputtering a surface that had been previously studied with Cs for times that were about 300% of that usually needed to remove impurities at the monolayer level. While most of the dosed Cs was rapidly removed by sputtering after Cs adsorption, this residual Cs could not be removed with additional sputtering times that were approximately tenfold longer than typically needed to remove a monolayer adsorbate from this sample, but its XPS signal instead only decreased by ~50%. This proves that this residual Cs was either present as a low concentration impurity dispersed deeply into the bulk, or in the form of thick domains which cover only a small fraction of the surface (perhaps as an oxide of Cs or a mixed Cs-Ti oxide). Annealing above 850 K sometimes caused a modest increase in this background Cs level. A good (1 × 1) LEED pattern characteristic of clean TiO₂(110) was obtained from annealed surfaces with the level of residual Cs depicted in curve *a* of Fig. 1, which further confirms such models. It was therefore concluded that this residual Cs was not greatly perturbing the properties of the clean TiO₂ surface, and it was reasonable to continue studying with this level of residual Cs on the "clean" surface. This was further confirmed by a few control experiments wherein the sputter cleaning was continued for much, much longer times, so as to decrease the Cs level to ~1/4 of that shown in curve *a* of Fig. 1.

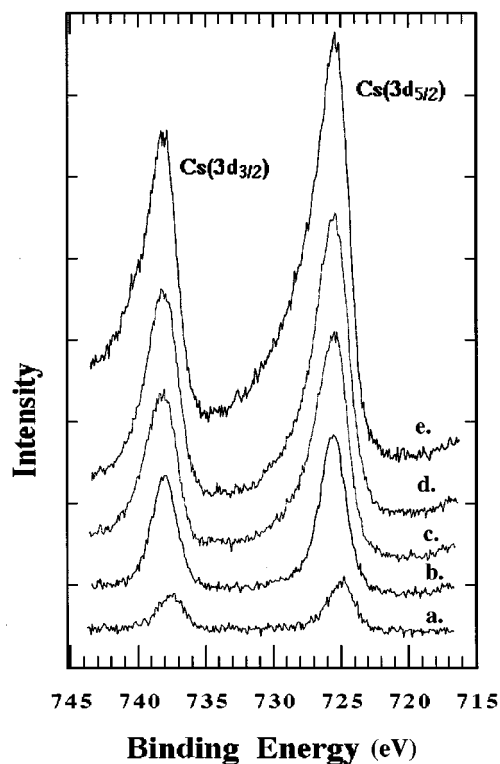


FIG. 1. Cs(3d) XPS spectra for different cesium coverages on TiO₂(110), collected with a pass energy of 100 eV using Al Kα radiation: curve *a*, residual "background" Cs signal on the nominally clean surface (see text), and after the vapor deposition of additional Cs; curve *b*, 0.51 ML, giving $I_{\text{Cs}}/I_{\text{Ti}}^0 = 0.795$; curve *c*, 0.99 ML, giving $I_{\text{Cs}}/I_{\text{Ti}}^0 = 1.53$; curve *d*, ~1.6 ML, giving $I_{\text{Cs}}/I_{\text{Ti}}^0 = 1.7$; curve *e*, ~7.5 ML giving $I_{\text{Cs}}/I_{\text{Ti}}^0 = 2.81$. These spectra were similar whether collected at room temperature or below down to 150 K, except that the higher Cs coverages (above 1 ML) could not be achieved except below ~250 K. Coverages were determined as described in Figs. 2 and 5.

Curves *b*–*e* of Fig. 1 show the growth of the Cs(3d) XPS peaks with increasing coverage during the vapor deposition of Cs into TiO₂(110). Both the Cs(3d_{5/2}) and Cs(3d_{3/2}) peaks start out as rather narrow lines, but at coverages approaching one monolayer and above, the peaks broadened rapidly to higher binding energy (BE), clearly indicating the presence of unresolved satellites at 2–6 eV higher BE than the main peak. This broadening is easily recognized as the growth of Cs plasmon loss satellites, since very similar broadening is observed at coverages approaching one monolayer and above during the vapor deposition of Cs onto transition-metal substrates.^{30,32,33} Their presence in the spectrum signals the onset of metallic Cs-Cs bonding.

The Ti(2p_{3/2}) peak was observed to decrease during Cs deposition as expected for overlayer growth. By one monolayer Cs coverage, the Ti peak intensity was attenuated by ~30% from its initial value. We define one monolayer (ML) of Cs (1.0 ML) by the appearance of the Cs multilayer peak in TPD (see below). At 1.0 ML coverage, the Cs(3d_{5/2}):Ti(2p_{3/2}) intensity ratio, $I_{\text{Cs}}/I_{\text{Ti}}$, was 2.2 (after subtracting the residual background Cs signal). The average ratio of this background-corrected Cs(3d_{5/2}) intensity at 1.0

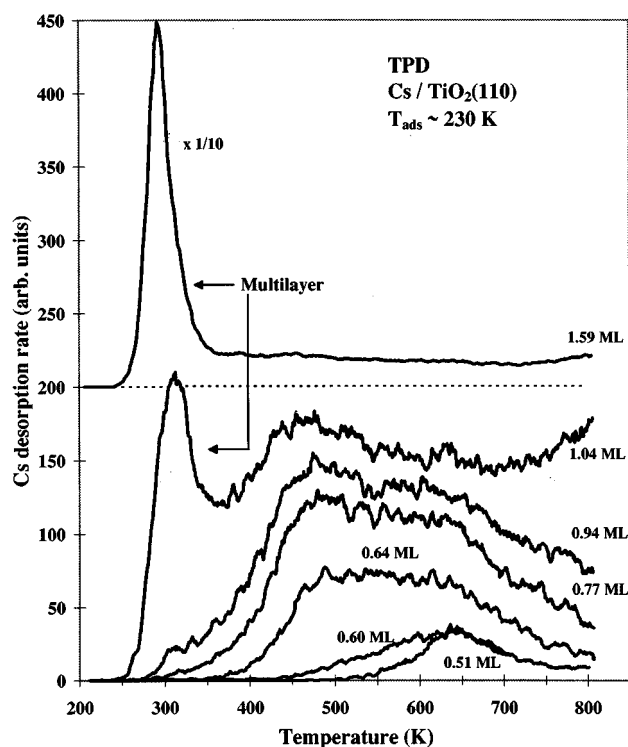


FIG. 2. Temperature-programmed desorption (TPD) curves for Cs desorption from $\text{TiO}_2(110)$ after adsorption at ~ 230 K. The curves are for increasing initial coverages of Cs as indicated. The completion of a monolayer is easily identified by the appearance of the sharp multilayer peak at ~ 300 K. Coverages below 1 ML were calculated from the XPS ratio, $I_{\text{Cs}}/I_{\text{Ti}}^0$, assuming it to be proportional to the dosed Cs coverage in this range. Coverages above 1 ML were calculated by comparing the multilayer TPD peak's area to the TPD peak area for 1 ML integrated up to 800 K, assuming that the latter corresponds to desorption of 50% of 1 ML of Cs (see text). The heating rate was constant at ~ 5 K/s.

ML to the $\text{Ti}(2p_{3/2})$ intensity of the initially clean surface, $I_{\text{Cs}}/I_{\text{Ti}}^0$ was 1.55. All Cs coverages below 1 ML reported here are based on this measured $I_{\text{Cs}}/I_{\text{Ti}}^0$ ratio, assuming that $I_{\text{Cs}}/I_{\text{Ti}}^0$ is proportional to Cs coverage, which it should be in the first ML.

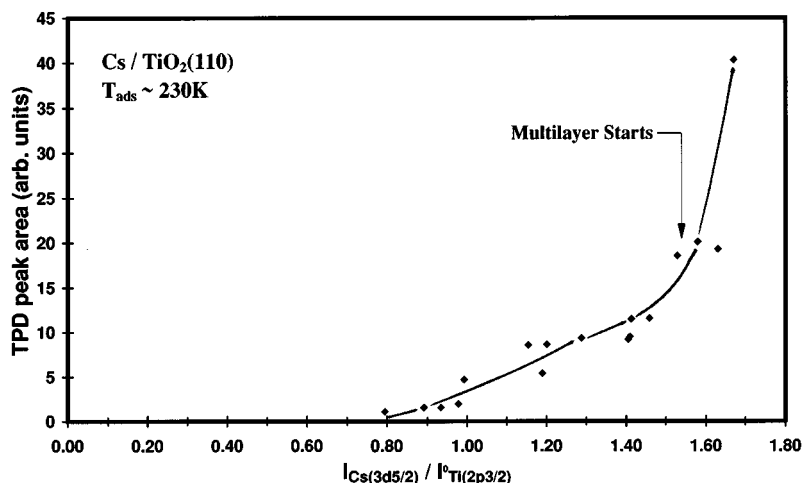


FIG. 3. Variation in the time-integrated Cs TPD peak intensity (below 800 K) versus the measured XPS ratio, $I_{\text{Cs}}/I_{\text{Ti}}^0$, of Cs vapor deposited onto $\text{TiO}_2(110)$ at ~ 230 K. This ratio is proportional to the added Cs coverage below 1 ML. The coverage where the onset of the multilayer TPD peak is observed, which we define as one monolayer, is indicated by the arrow.

The $\text{Ti}(2p)$ peaks broadened considerably toward lower binding energy upon Cs adsorption, very similar to that seen by Hardman *et al.*⁸ upon K adsorption on $\text{TiO}_2(100)$. Consistent with their explanation, we attribute this to the growth of an unresolved peak at ~ 1.6 eV lower binding energy due to the creation of Ti^{3+} ions in the surface. That is, the alkali metal is partially reducing the oxide substrate, as it becomes at least partially oxidized. This increase in Ti^{3+} intensity reached its maximum effect by $\sim \frac{1}{2}$ to $\frac{3}{4}$ ML coverage, and corresponded to $\sim 10\%$ of the Ti^{4+} intensity. Since the mean free path of the Ti photoelectrons through TiO_2 is ~ 31 Å, this 10% corresponds to ~ 3 Å thickness, equivalent to the reduction of all Ti ions in the topmost atomic plane to Ti^{3+} . Similar results were also observed during Na adsorption on this same surface.²

The thermal desorption of Cs from $\text{TiO}_2(110)$ following adsorption at ~ 230 K is shown in Fig. 2 as a function of increasing Cs coverage. The sharp peak at 300 K in the highest coverage spectra is due to multilayer Cs, and is seen at this same temperature in the TPD of Cs from transition-metal surfaces as well.³⁰ It did not saturate with further increasing coverage up to 7.5 ML. We define one monolayer here as the Cs coverage necessary to just give the onset of the appearance of this multilayer TPD peak, averaged over several TPD series like that shown in Fig. 2. This occurred at an average value of the XPS ratio, $I_{\text{Cs}}/I_{\text{Ti}}^0$ of 1.55. Starting from the lowest submonolayer coverages shown, there is a continuous population of desorption intensity from the highest temperature probed (~ 800 K) to increasingly lower temperature as Cs coverage increases. This reflects a nearly continuous decrease in desorption energy, and therefore adsorption energy, with coverage.

The time-integrated Cs TPD peak area (below 800 K) for adsorption at ~ 230 K is plotted as a function of the Cs/Ti XPS ratio, $I_{\text{Cs}}/I_{\text{Ti}}^0$ in Fig. 3. As can be seen, no desorption is seen below 800 K for initial Cs coverages below $\sim \frac{1}{2}$ ML. The adsorption energy at coverages below $\frac{1}{2}$ ML was clearly too high to be probed by TPD. Above $\sim \frac{1}{2}$ ML of Cs, the TPD peak intensity appeared and grew. At coverages approaching and above 1 ML, the TPD peak area increased rather nonlinearly with increasing XPS ratio, $I_{\text{Cs}}/I_{\text{Ti}}^0$ ratio, as shown. With these higher initial Cs coverages, about half of a Cs monolayer remained on the surface after the TPD.

The $I_{\text{Cs}}/I_{\text{Ti}}^0$ ratio was only 2.81 after adsorption of ~ 7.5 ML of Cs, which should give a desorption peak area of ~ 260 in the units of Fig. 3. This point is not entered there since the TPD peak went off scale, so it was not properly recorded. Nevertheless, this result proves that the $I_{\text{Cs}}/I_{\text{Ti}}^0$ ratio in XPS increases only very slowly with Cs coverage above 1 ML compared to below 1 ML. This trend is also obvious already from the last points in Fig. 3. We attribute the slow growth of the $I_{\text{Cs}}/I_{\text{Ti}}^0$ ratio above 1 ML to a Stranski-Krastanov growth mode. That is, whereas the first Cs monolayer spreads uniformly across the surface, higher Cs coverages agglomerate into three-dimensional (3D) clusters of pure, metallic Cs that are much thicker than the probe depth of XPS and cover only a very small fraction of the surface. These 3D cluster of Cs contribute little to the XPS signal of Cs, yet they hold large amounts of the dosed Cs.

The TPD of Fig. 2 were only obtained if the alkali-metal covered surface was not allowed to sit for too long above ~ 200 – 250 K before TPD. If it did sit for too long at too high a temperature, desorption intensity decreased in the regions shown (including the multilayer peak), apparently shifting into higher-temperature regions which were inaccessible by TPD (above 800 K). The onset of this shifting can be seen in the increasing high-temperature tails in the top two TPD spectra of Fig. 2. Note that the Cs desorption intensity at 800 K was $\sim 20\%$ higher in the curve for 1.59 ML than in the 1.04-ML curve of Fig. 2, when compared on the same scale. This growth in high-temperature intensity may be due to the slow conversion of the alkali-metal monolayer into another more stable form, such as a Cs oxide or a mixed Cs/Ti oxide. Note that the heat of formation of Cs₂O is -345 kJ/mol, very close to the energy cost to reduce TiO₂ fully to Ti₂O₃ (368 kJ/mol of O).³⁴ Thus, while full bulk reduction of TiO₂ to Ti₂O₃ by Cs is not expected to be thermodynamically favored,¹ some partial bulk reduction (i.e., creating more bulk oxygen vacancies as the Cs oxidizes) could easily be thermodynamically downhill. As this would require some time for diffusion through the bulk, this may be a kinetically limited process. Furthermore, since mixed oxides of titanium with alkali metals (e.g., Na₂Ti₂O₅, K₂Ti₂O₅, and Na₂Ti₆O₁₃) are known to be stable, the formation of such a mixed Cs-Ti oxide may be thermodynamically favored even in the bulk, but kinetically limited here. The formation of such a mixed oxide would also explain the residual Cs that could not be removed by sputtering unless done for much, much longer times.

If the adsorption of Cs was performed in insufficient vacuum, or if the waiting time in vacuum was too long after Cs deposition, an impurity peak also complicated the TPD spectrum. This impurity peak was characterized by the near-simultaneous desorption of an additional, sharp peak for Cs and a peak for CO₂, both at ~ 600 K. This is similar to the peak observed after dosing CO₂ to Cs on Cu(110), where both CO₂ and Cs were observed to desorb nearly simultaneously upon the decomposition of a Cs carbonate species.³⁰ Its peak temperature was ~ 660 K for multilayer Cs coverages on Cu(110), but depended upon the Cs coverage at lower coverages.

Work-function and band-bending changes measured as a function of Cs coverage during deposition at 300 K are shown in Fig. 4. These data indicate that the alkali metal

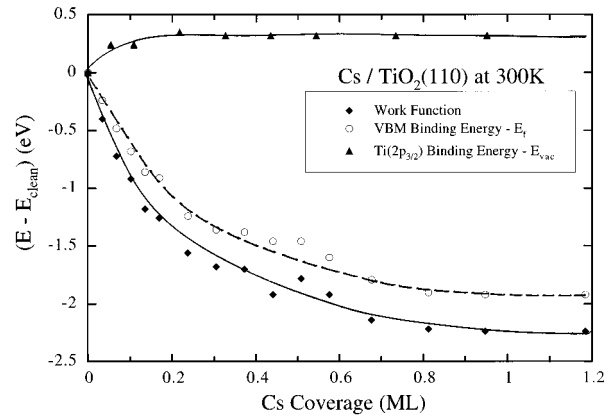


FIG. 4. Variations with Cs coverage in the work function ($\Delta\phi$) and the binding energy of the Ti($2p_{3/2}$) peak relative to the Fermi level (E_F) during deposition at 300 K onto TiO₂(110). The latter value reflects the long-range Cs-induced band bending (BB). Also shown is the sum of these two curves, which gives the Cs-induced shift in the position of the valence-band maximum (VBM) relative to the vacuum level (E_{vac}), since all the bands shift together. The slope of this VBM or sum curve is directly proportional to the local surface dipole moment due to adsorbed Cs. Here, Cs coverages were estimated from the XPS ratio, $I_{\text{Cs}}/I_{\text{Ti}}^0$ ratio, assuming it to be proportional to coverage in the region measured here.

adsorbs ionically up to relatively high coverages. Band bending often occurs upon adsorption on semiconductors, and is measured by following the shift in substrate core levels with respect to the Fermi level (spectrometer reference).^{1,24,25,35} Here we used the observed shifts in the Ti($2p_{3/2}$) peak center to monitor band bending. As can be seen, the smallest added Cs coverages cause this peak to shift to higher binding energy with respect to the bulk Fermi level by ~ 0.2 eV, reflecting a downward bending of the bands of TiO₂ moving from the bulk toward the surface. This shifting saturates rapidly with Cs coverage at ~ 0.3 eV, and the majority of this shift occurred by $\sim 5\%$ of a ML.

Band bending (BB) is an electrostatic effect which reflects the influence of surface charge on the electronic energy levels (bands) of the substrate. This charge influences the energies of all levels equally, so the measured core-level shifts also reflect the shifts in the oxide's valence band and its conduction band. Of course, this charge does not affect these orbital (band) energies deep in the bulk of semiconducting oxides such as this, since they are screened out by the conduction electrons (or hole-type charge carriers) over a depth comparable to the Thomas-Fermi charge screening length (typically on the order of 10^{-6} to 10^{-8} m).^{1,24,26,35} This is the length over which the bands ‘‘bend.’’ This screening is accomplished by an increase or decrease in the conduction electron density in response to the surface charge, and therefore the development of a space-charge layer which also extends to this same depth. Since XPS probes a depth small compared to this, only the fully bent (i.e., near-surface) energies are measured.

As shown in Fig. 4, the work function decreases strongly upon Cs addition, ultimately by ~ 2.2 eV. Most of this decrease occurs in the first $\frac{1}{4}$ ML, and the decrease is almost saturated by $\frac{1}{2}$ ML.

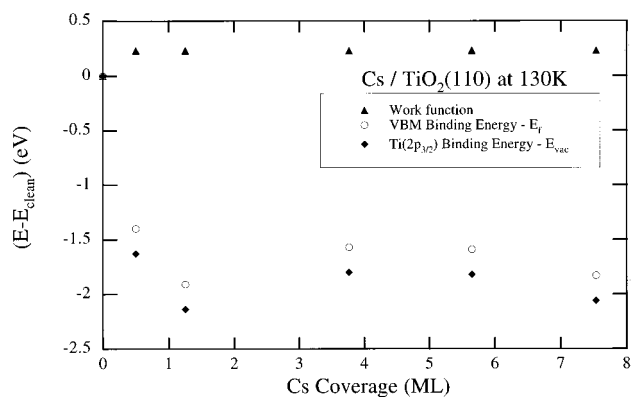


FIG. 5. As in Fig. 4, except for a substrate held at 130 K. Note that the trends are the same as at 300 K, except that multilayer coverages could be achieved at this lower temperature. Here, Cs coverages below 1 ML were estimated from the XPS ratio, $I_{\text{Cs}}/I_{\text{Ti}}^0$, assuming it to be proportional to coverage in that region. Coverages above 1 ML were estimated by assuming that the Cs coverages was proportional to Cs deposition time. The accuracy of this assumption ($\sim \pm 20\%$) was tested in control experiments at ~ 300 K using XPS ratios and only coverages below 1 ML.

The sum of the work-function and band-bending curves is also shown in Fig. 4. The slope of this band-bending-corrected work function, or sum, curve directly reflects changes in the *local* surface dipole layer.^{24–26} This is exactly what is measured by work-function changes *alone* on metal substrates, so it can be interpreted in the same way that adsorbate-induced work-function changes are interpreted on metallic surfaces. Thus the magnitude of the slope of this sum curve gives the local dipole moment for the adsorbate-substrate complex, using the Helmholtz equation.^{36–38} The large initial slope corresponds to a dipole moment of ~ 6 D for the Cs-substrate complex, indicating strong electron transfer from Cs into the nearby atoms of the oxide lattice. At higher coverages the slope gradually decreases, ultimately to zero by about 1 ML. This shows that the adsorption gradually converts from ionic to neutral as coverage increases in the first ML, reminiscent of what is observed for alkali metals on transition-metal surfaces.^{36–39} This is due to mutual depolarization as the parallel dipoles pack closer and closer

together, and reflects the polarizability of the adsorbate-substrate complex.^{36,38,39} This depolarization here on TiO_2 is, however, not as strong as on metal surfaces, since in the latter case the slope actually reverses at high coverages.^{30,36–39} The average slope over the first $\frac{1}{4}$ -ML coverage corresponds to a dipole moment of ~ 3 D per adsorbed Cs, indicating that there is strong charge transfer even up to moderate coverages.

Note that Fig. 4 extends to a coverage of almost 1.2 ML, as estimated here by assuming the XPS ratio, $I_{\text{Cs}}/I_{\text{Ti}}^0$, was proportional to coverage in this range. The TPD data (Fig. 2) show that coverages above 1 ML should not be stable at 300 K. The fact that we were able to achieve Cs/Ti XPS ratios corresponding to >1 ML in this experiment, which took much longer than a simple TPD, can be attributed to the slow conversion of a small part of Cs into the high-temperature forms (Cs oxide or Cs-Ti mixed oxide), as also suggested by other results above.

Work-function changes versus Cs coverage were also measured for an adsorption temperature of 240 K, up to ~ 0.9 ML Cs. The results were almost exactly the same as shown for adsorption at 300 K in Fig. 4, so they are not presented here.

Figure 5 shows similar curves for the work function and band bending as in Fig. 4, except that these were measured during adsorption at 130 K, and therefore multilayer coverages could be achieved. Again, the general trends below 1 ML are the same at 130 and 300 K. At higher coverages, the curves are nearly constant, although the work function appears to first increase slightly and then decrease. From the saturation value of the work-function change, ~ -2.2 eV, we might crudely estimate by summing values that the clean $\text{TiO}_2(110)$ surface has a work function of ~ 4.3 – 4.4 eV, since bulk Cs has a work function of ~ 2.14 eV.³⁴ The work function of clean $\text{TiO}_2(110)$ has previously been reported to be 5.3–5.5 eV, based on several reports,⁴⁰ with other more recent measurements of 5.02 eV (Ref. 41) and 6.83 eV. (Ref. 42). The estimate above based on simple summing may be inaccurate due to the Stranski-Krastanov growth mode here. The fact that Cs clusters into 3D islands that cover only a small fraction of the surface (see above) means that the saturation work function should really be a geometric average of the work function of bulk Cs (on the 3D Cs patches) and that

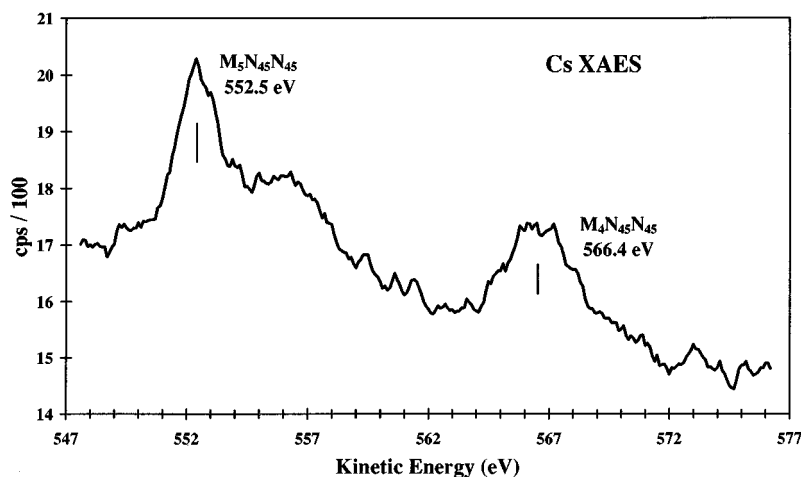


FIG. 6. X-ray-excited Auger spectrum of Cs (MNN) peaks for the residual background Cs present in low concentration after extensive sputtering and annealing.

of 1 ML of Cs, covering most of the surface.

In order to better characterize the residual “background” Cs that could not be easily cleaned from the sample (curve *a* in Fig. 1), we present in Fig. 6 its x-ray excited AES spectrum (XAES), for the energy region of the Cs(*MNN*) lines. Here, Al *K*α x-ray excitation was used. It should be noted that this residual Cs became more and more difficult to remove to acceptable levels as experiments with Cs proceeded, until finally further experiments with that crystal became impossible to continue without replacing the sample (or possibly by mechanically polishing it again, which we did not attempt).

IV. DISCUSSION

Rodriguez, Clendening, and Campbell³⁰ have studied Cs adsorption on Cu(110) in this same apparatus, where the close-packed monolayer coverage was clearly identified by both TPD and work-function measurements. That close-packed monolayer, which was shown by LEED to correspond to an absolute coverage of 5.2×10^{14} Cs atoms per cm², showed a Cs(*3d*_{5/2}):Cu(*2p*_{3/2}) intensity ratio, I_{Cs}/I_{Cu} of 0.13. The ratio of its Cs(*3d*_{5/2}) intensity to the Cu(*2p*_{3/2}) intensity from the clean Cu surface, I_{Cs}/I_{Cu}^0 , was 0.11, also using this same apparatus and Al *K*α x rays. Note that a hypothetical monolayer of Cs on TiO₂(110) containing one Cs adatom per unit cell of TiO₂(110) would also correspond to this same packing density, or 5.2×10^{14} (Cs adatoms) cm⁻². Thus one might expect a very similar absolute XPS signal for the Cs monolayer here. The Cs(*3d*_{5/2}):[clean Ti(*2p*_{3/2})] intensity ratio one would expect from such an overlayer can easily be calculated using the known I_{Cs}/I_{Cu}^0 ratio for this same packing density on Cu(110), corrected by the ratio of Cu(*2p*_{3/2}):Ti(*2p*_{3/2}) signals expected for the pure bulk substrates, I_{Cu}^0/I_{Ti}^0 . The ratio I_{Cu}^0/I_{Ti}^0 can be estimated from the bulk XPS Cu:Ti sensitivity ratio, 4.2:1.2,⁴³ and the ratio of the packing density of Cu atoms in bulk Cu to that of Ti atoms in bulk TiO₂, (8.46×10^{22} cm⁻²):(3.2×10^{22} cm⁻²). Thus one expects a ratio

$$\begin{aligned} I_{Cs}/I_{Ti}^0 &= 0.11(4.2/1.2)(8.46 \times 10^{22} \text{cm}^{-2}/3.21 \times 10^{22} \text{cm}^{-2}) \\ &= 1.02. \end{aligned}$$

This compares reasonably well with the measured ratio of 1.55 for what we define as one monolayer of Cs on TiO₂ based on TPD, especially given the possibilities for intensity changes associated with photoelectron diffraction effects, and expected inaccuracies in relative sensitivity factors.

One can also estimate the percentage attenuation of the Ti(*2p*_{3/2}) intensity expected for such a monolayer. This packing density of 5.2×10^{14} (Cs adatoms) cm⁻² corresponds to a Cs overlayer thickness of 6.1 Å, based on the packing density of bulk Cs, 8.47×10^{21} cm⁻³. An overlayer of this thickness should attenuate the Ti(*2p*_{3/2}) intensity by 26%, given the mean free path of these electrons through Cs of 20 Å.⁴⁴ This is very close to the value of ~30% observed.

In conclusion, the absolute XPS intensities of 1.0 ML of Cs are consistent with a packing density of

$\sim 5.2 \times 10^{14}$ cm⁻², or about one Cs adatom per unit cell. Given the error bars on the electron mean free paths and sensitivity factors used in the above calculations, one should recognize that Cs packing densities between about 4×10^{14} and 8×10^{14} cm⁻² would also be consistent with the XPS signals observed. This may be achieved by first filling the troughs with rows of Cs ions (at a coverage less than one per unit cell), followed by adsorption of more neutral Cs adatoms on top of the rows of bridging oxygen anions of the lattice. This would be consistent with the conversion from cationic to neutral adsorption suggested by the XPS, work-function, and band bending measurements and by TPD.

Similar work-function curves to that shown in Figs. 4 and 5 have been measured for other alkali-metal adsorption on several semiconducting oxides,^{2,10,15,17} through in those cases the authors did not correct for band bending, which is needed in order for the local surface dipole to be accurately determined. Nevertheless, band bending is usually only a few tenths of a volt when measured,¹ so the general picture one gets from those results is similar to that outlined above: highly cationic adsorption up to $\frac{1}{4}$ to $\frac{1}{2}$ ML followed by mutual depolarization which is complete by 1 ML, and nearly complete somewhat above $\frac{1}{2}$ ML.

As we saw in Fig. 4, the adsorption of small amounts of Cs on TiO₂(110) also causes downward band bending, although this effect nearly saturates with the lowest coverage measured. Band-bending changes for such semiconductor oxides often results from Fermi level pinning within the band gap by adsorbate-induced surface states or adsorbate-induced occupation of surface states, and the resulting surface charge.^{1,24-26,35} On semiconductors, it is common for the first few percent of a metal monolayer to cause large amounts of band bending due to the creation of surface electronic states.^{1,25,35,45} At low coverages the position is controlled by the equilibrium between charge in the depletion layer and donor-type surface states induced by the adsorbate. For some semiconductors, it has been shown that the position in the band gap of these adsorbate-induced donor states varies linearly with the ionization energy of the free metal atom.³⁵ Thus they should be quite high-lying states for an alkali metal like Cs. Band bending can be nearly saturated after only a tiny metal coverage because the concentration of dopant (oxygen vacancies here) within the depth of band bending (approximately 0.01 to 1.0 micrometer range) is typically less than $\sim 10^{13}$ /cm², so that the number of electrons needed to dramatically change carrier concentrations in this space-charge layer is tiny.^{25,35,40} This explains why the band bending nearly saturates after the lowest coverage dose of Cs on TiO₂(110) in Figs. 4 and 5.

The direction of the initial band bending in Figs. 4 and 5 again suggests a cationic character for Cs on TiO₂(110), since metal-induced surface states are generally interpreted to be of donor character when band bending is downward.^{25,35,45} At low coverages, the electron density donated by the alkali metal can partially go deep into the space-charge layer of the TiO₂, causing band bending, whereas at higher coverages it appears to be only localized at the surface atoms of the oxide lattice, causing a local surface dipole layer. This local surface dipole layer is being created at low coverages as well, and it is in fact most strongly produced at the lowest Cs coverages. The appearance of Ti³⁺ intensity in

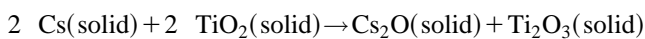
the $Ti2p_{3/2}$ (XPS) line after low coverage doses of Cs is also clear evidence of local charge transfer from the Cs adatoms to Ti ions in the topmost layer of the substrate.

As shown in Fig. 2, there is a continuous population of desorption intensity to increasingly lower temperature as Cs coverage increases. This reflects a nearly continuous decrease in desorption energy, and therefore adsorption energy. For coverages below $\frac{1}{2}$ ML, the desorption peak temperature is clearly somewhere above 800 K. Using a first-order desorption rate law and assuming a typical prefactor for desorption of 10^{13} s^{-1} , simple Redhead analysis⁴⁶ of an 800-K TPD peak temperature gives a desorption energy 208 kJ/mol. Clearly, the first $\sim\frac{1}{2}$ ML must be bound even more strongly than this. Thus Fig. 2 indicates a desorption energy for Cs which decreases continuously with coverage from >208 kJ/mol down to the vaporization energy of pure Cs, 78 kJ/mol,³⁴ at monolayer coverage. Such a dramatic and smooth decrease in adsorption energy with coverage is also typically observed for alkali metals on metal surfaces, where it is attributed to increasing dipole-dipole repulsions as the adsorbates pack closer and closer together.^{36,38,39} These repulsions lead to mutual depolarization of the alkali-metal adsorption complexes with increasing coverage within the first monolayer on metals.^{36,38,39} This also occurs on oxide surfaces, as judged by the decrease in local dipole moment with coverage seen in Fig. 4, and observed on other oxides (see above).

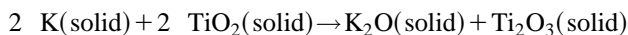
Similar TPD spectra and work-function changes with coverage have also been reported for Cs and K adsorption on Si(100) and (111) surfaces,^{39,47-51} where a rapid decrease in adsorption energy (desorption temperature) also accompanies the decrease in slope of the work-function curve. Again, these have been attributed to partially ionic adsorption and changes in polarization with coverage, although some authors suggest a more covalent bonding model on Si(100) than on Si(111).⁵²

We noted above that the high coverage TPD spectra of Fig. 2 were sensitive to the waiting time before desorption if the sample temperature was not far below room temperature. Similar effects are suggested by reviewing the literature with respect to TPD studies of alkali metals on other oxides. The TPD spectrum after 3 ML of K adsorbed onto $TiO_2(110)$ was reported by Hayden and Nicholson.⁶ It showed a high-temperature K desorption peak at ~ 750 K, and a series of low-temperature peaks between 300 and 370 K. The high-temperature peak was associated with a stable $c(2 \times 2)$ -K overlayer. Most of the low-temperature peaks were considered to be slightly perturbed from the multilayer bulk K peak, which should appear at ~ 325 K. However, another study of this same system showed quite a different behavior.⁵ In that case, K_2O multilayers (heat of formation equal to -362 kJ/mol) were grown during deposition of K onto $TiO_2(110)$, and no metallic potassium was seen even after very large K doses.⁵ In that case the potassium oxide was reported to be stable up to 900 K. It seems that some other variable, namely, the time scale of the experiment, may be quite important in these systems.

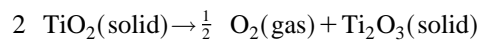
Note that the bulk reactions



and



are almost thermoneutral at room temperature, since the standard enthalpy of formation of Cs_2O is -345 kJ/mol and that of K_2O is -362 kJ/mol,³⁴ whereas the standard enthalpy of the reaction



is $+368$ kJ/mol.³⁴ Therefore *partial* reduction of the TiO_2 by adsorbed K and Cs (i.e., production of a higher concentration of bulk O vacancies), or formation of a mixed alkali-metal-Ti oxide may well be thermodynamically downhill. Consequently, the influence of time may be related to the slow kinetics of these bulk reactions.

Desorption of K from $\text{NiO}(100)$ only showed a TPD doublet peak at ~ 800 and 1000 K which never saturated with K dose, and never any lower-temperature states due to metallic K.¹⁷ The lack of saturation suggests that these high-temperature peaks probably reflect the decomposition of some multilayer potassium oxide or mixed-metal/alkali-metal oxide, rather than desorption of K from sites on the oxide. Since the heat of formation of potassium oxide (-362 kJ/mol) is much larger than nickel oxide (-240 kJ/mol), bulk reduction of the NiO by K is fully expected thermodynamically, consistent with this picture. A later study of this same system showed only a single TPD peak for K at ~ 760 K even up to 2.5 ML coverage, and high-resolution electron-energy-loss spectroscopy (HREELS) evidence for extensive formation of K—O bonds,¹⁹ again suggesting multilayer alkali-metal oxide formation and substrate reduction.

In a TPD study of Cs on $\text{NiO}(100)$,²⁰ a doublet for Cs was also seen at ~ 800 and 1000 K. The similarity to K on $\text{NiO}(100)$ (see above) is surely related to the similarity in the heats of their oxide formations: 345 kJ/mol for Cs, 362 kJ/mol for K.³⁴

Well-ordered overlayers are frequently reported upon alkali-metal adsorption on oxide surfaces.¹ For example, a $c(2 \times 2)$ overlayer of potassium has been observed on the $\text{TiO}_2(110)$ surface after annealing to 650–750 K,⁶ which corresponds to at least one K adatom per every two unit cells. A $c(4 \times 2)$ is seen after Na adsorption on this same face.² A $c(2 \times 2)$ overlayer of potassium has also been observed on the $\text{TiO}_2(100)$ surface,⁹ and the adsorption site has been derived from SEXAFS data by Thornton and co-workers.⁹ We were unable to monitor for LEED structures of the Cs adlayer, but one would certainly expect ordered structures at coverages up to $\sim\frac{1}{2}$ ML, based on these prior studies. This would be the coverage regime where we suggest Cs is probably adsorbing into sites along the troughs of the $\text{TiO}_2(110)$ surface.

ACKNOWLEDGMENTS

The authors would like to acknowledge support for this work by the Department of Energy, Office of Basic Energy Sciences, Chemical Sciences Division. They thank Lara Gamble for much technical assistance, and useful discussions. A. W. G. thanks the Research Experience for Undergraduates Program of the National Science Foundation for financial support during part of this work.

- ¹C. T. Campbell, Surf. Sci. Rep. (to be published).
- ²H. Onishi, T. Aruga, C. Egawa, and Y. Iwasawa, Surf. Sci. **199**, 54 (1988).
- ³J. Nerlov, Q. Ge, and P. Möller, Surf. Sci. **348**, 28 (1996).
- ⁴P. W. Murray, N. G. Condon, and G. Thornton, Surf. Sci. **323**, 281 (1995).
- ⁵R. J. Lad and L. S. Dake, in *Structure and Properties of Interfaces in Materials*, edited by W. A. T. Clark, U. Dahmen, and C. L. Briant, MRS Symposia Proceedings No. 238 (Materials Research Society, Pittsburgh, 1992), pp. 823–828.
- ⁶B. E. Hayden and G. P. Nicholson, Surf. Sci. **274**, 277 (1992).
- ⁷D. Purdie, B. Riehl, M. Tschudy, A. Thomas, P. J. Hardman, C. A. Muryn, and G. Thornton, J. Phys. (France) IV **C9**, 163 (1994).
- ⁸P. J. Hardman, R. Casanova, K. Prabhakaran, C. A. Muryn, P. L. Wincott, and G. Thornton, Surf. Sci. **269/270**, 677 (1992).
- ⁹K. Prabhakaran, D. Purdie, R. Casanova, C. A. Muryn, P. J. Hardman, P. L. Wincott, and G. Thornton, Phys. Rev. B **45**, 6969 (1992).
- ¹⁰R. Casanova, K. Prabhakaran, and G. Thornton, J. Phys. Condens. Matter **3**, S91 (1991).
- ¹¹D. Purdie, C. A. Muryn, S. Crook, P. L. Wincott, G. Thornton, and D. A. Fischer, Surf. Sci. **290**, L680 (1993).
- ¹²P. A. Taylor and B. J. Hopkins, J. Phys. C **11**, L643 (1978).
- ¹³R. Leysen, B. J. Hopkins, and P. A. Taylor, J. Phys. C **8**, 907 (1975).
- ¹⁴H.-J. Freund, B. Dillmann, D. Ehrlich, M. Haßel, R. M. Jaeger, H. Kühlenbeck, C. A. Ventrice, Jr., F. Winkelmann, S. Wohrab, and C. Xu, J. Mol. Catal. **82**, 143 (1993).
- ¹⁵T. Rogelet, S. Soederholm, M. Qvarford, N. L. Saini, U. O. Karlsson, I. Lindau, and S. A. Flodstroem, Solid State Commun. **85**, 657 (1993).
- ¹⁶C. A. Ventrice, Jr., D. Ehrlich, E. L. Garfunkel, B. Dillmann, D. Heskett, and H. J. Freund, Phys. Rev. B **46**, 12 892 (1992).
- ¹⁷S. Kennou, M. Kamaratos, and C. A. Papageorgopoulos, Vacuum **41**, 22 (1990).
- ¹⁸J. G. Chen, M. D. Weisel, F. M. Hoffmann, and R. B. Hall, Amer. Chem. Soc. Symp. Ser. **523**, 133 (1993).
- ¹⁹J. G. Chen, M. D. Weisel, J. H. Hardenbergh, F. M. Hoffmann, C. A. Moms, and R. B. Hall, J. Vac. Sci. Technol. A **9**, 1684 (1991).
- ²⁰S. Kennou, M. Kamaratos, and C. A. Papageorgopoulos, Surf. Sci. **256**, 312 (1991).
- ²¹M. Bender, K. Al-Shamery, and H.-J. Freund, Langmuir **10**, 3081 (1994).
- ²²H. Onishi, C. Egawa, T. Aruga, and Y. Iwasawa, Surf. Sci. **191**, 479 (1987).
- ²³P. W. Murray, N. G. Condon, and G. Thornton, Surf. Sci. **323**, L281 (1995).
- ²⁴P. Zurcher and R. S. Bauer, J. Vac. Sci. Technol. A **1**, 695 (1983).
- ²⁵K. H. Ernst, A. Ludviksson, R. Zhang, J. Yoshihara, and C. T. Campbell, Phys. Rev. B **47**, 13 782 (1993).
- ²⁶W. Göpel, Prog. Surf. Sci. **20**, 9 (1985).
- ²⁷J. M. Campbell, S. G. Seimanides, and C. T. Campbell, J. Phys. Chem. **93**, 815 (1989).
- ²⁸M. B. Hugenschmidt, L. Gamble, and C. T. Campbell, Surf. Sci. **302**, 329 (1994).
- ²⁹L. Gamble, M. B. Hugenschmidt, C. T. Campbell, T. A. Jurgens, and J. W. Rogers, J. Am. Chem. Soc. **115**, 12 096 (1993).
- ³⁰J. A. Rodriguez, W. D. Clendening, and C. T. Campbell, J. Phys. Chem. **93**, 5238 (1989).
- ³¹C. T. Campbell, Crit. Rev. Surf. Chem. **3**, 49 (1994).
- ³²S. A. Lindgren and L. Walden, Phys. Rev. B **22**, 5967 (1980).
- ³³B. M. Hartley, Phys. Lett. A **24**, 396 (1967).
- ³⁴*CRC Handbook of Chemistry and Physics*, edited by D. R. Lide (CRC Press, Boston, 1990).
- ³⁵W. Mönch, Rep. Prog. Phys. **53**, 221 (1990).
- ³⁶C. T. Campbell, Annu. Rev. Phys. Chem. **44**, 775 (1990).
- ³⁷L. Schmidt and R. Gomer, J. Chem. Phys. **42**, 3573 (1965).
- ³⁸R. L. Gerlach and T. N. Rhodin, Surf. Sci. **19**, 403 (1970).
- ³⁹*Physics and Chemistry of Alkali Metal Adsorption*, edited by H. P. Bonzel, A. M. Bradshaw, and G. Ertl (Elsevier, Amsterdam, 1989).
- ⁴⁰V. E. Henrich and P. A. Cox, *The Surface Science of Metal Oxides* (Cambridge University Press, Cambridge, England, 1994).
- ⁴¹A. K. See and R. A. Bartynski, Phys. Rev. B **50**, 12 064 (1994).
- ⁴²D. Vogtenhuber, R. Podloucky, A. Neckel, S. G. Steinemann, and A. J. Freeman, Phys. Rev. B **49**, 2099 (1994).
- ⁴³C. D. Wagner, J. Electron Spectrosc. Relat. Phenom. **32**, 99 (1983).
- ⁴⁴S. Tanuma, C. J. Powell, and D. R. Penn, Surf. Interface Anal. **17**, 911 (1991); **17**, 927 (1991).
- ⁴⁵S. V. Didziulis, K. D. Butcher, S. L. Cohen, and E. I. Solomon, J. Am. Chem. Soc. **111**, 7110 (1989).
- ⁴⁶P. A. Redhead, Vacuum **12**, 203 (1962).
- ⁴⁷C. Papageorgopolous and M. Kamaratos, Surf. Sci. **221**, 263 (1989).
- ⁴⁸M. Kamaratos, S. Kennou, and C. Papageorgopolous, Surf. Sci. **227**, 43 (1990).
- ⁴⁹G. Boishin and L. Surnev, Surf. Sci. **273**, 301 (1992).
- ⁵⁰G. Boishin, M. Tikhov, M. Kiskinova, and L. Surnev, Surf. Sci. **261**, 224 (1992).
- ⁵¹M. Nishijima, S. Tanaka, N. Takagi, and M. Onchi, Surf. Sci. **242**, 498 (1991).
- ⁵²P. S. Mangat and P. Soukiassian, Phys. Rev. B **52**, 12 020 (1995).